CONFIDENTIAL

Copy
RM H54I27

NACA RM H54I27

NACA

RESEARCH MEMORANDUM

LATERAL MOTIONS ENCOUNTERED WITH THE DOUGLAS D-558-II ALL-ROCKET RESEARCH AIRPLANE DURING EXPLORATORY FLIGHTS TO A MACH NUMBER OF 2.0

By Herman O. Ankenbruck and Chester H. Wolowicz

High-Speed Flight Station
Edwards, Calif.

CLASSIFIED DOCUMENT

NATIONAL ADVISORY COMMITTEE
FOR AERONAUTICS

WASHINGTON

December 17, 1954

CONFIDENTIAL

NATIONAL ADVISORY COMMITTEE FOR AERONAUTICS

RESEARCH MEMORANDUM

LATERAL MOTIONS ENCOUNTERED WITH THE DOUGLAS D-558-II ALL-ROCKET RESEARCH AIRPLANE DURING EXPLORATORY FLIGHTS TO A MACH NUMBER OF 2.0

By Herman O. Ankenbruck and Chester H. Wolowicz

SUMMARY

Flight tests were performed with the Douglas D-558-II research airplane in order to determine the lateral handling characteristics in straight flight at supersonic speeds. This paper primarily describes the lateral motions obtained at moderate and low angles of attack during a preliminary survey in pushovers and straight flight at supersonic Mach numbers up to about 2.0 at altitudes between 50,000 and 70,000 feet. Calculated lateral dynamic characteristics for level-flight conditions and some results of measurements of the effects of power on the rudder hinge moments are also included.

Based on these tests and calculations, it appears that the objectionable lateral dynamic stability characteristics as evidenced by difficulty of control due to poor damping characteristics, decreasing directional stability, and high ratios of roll to yaw are mostly caused by the low inclination of the principal axis relative to the flight path at the low angles of attack at which most of the flights were made, by the general deterioration of the important stability derivatives with increasing Mach number, and by the large ratio of I_X to I_Z. High ratios of rocket exhaust pressure to static pressure created large changes in rudder hinge-moment characteristics; however, the effect of power on the overall lateral handling qualities appears to be negligible.

INTRODUCTION

The National Advisory Committee for Aeronautics is conducting flight research at transonic and supersonic speeds using research-type aircraft at the NACA High-Speed Flight Station at Edwards Air Force Base, Calif. The Douglas D-558-II airplanes were obtained for the NACA by the Navy

Department in order to conduct flight research on swept-wing airplanes at high speeds. At the present time two D-558-II airplanes with different mass characteristics are being used in this program, one powered by a turbojet engine and a rocket engine and one powered by a rocket engine only. Both airplanes are launched at an altitude of about 30,000 feet from a Boeing B-29 airplane. The present paper describes the results obtained from the all-rocket airplane only.

Previous investigations have shown that poor dynamic lateral stability characteristics are frequently experienced with highly loaded airplanes at high speeds and high altitudes, and reference 1 shows that the airplane has poor dynamic stability characteristics at subsonic speeds in the landing configuration. It is the purpose of the present paper to describe briefly some of the results obtained with the all-rocket D-558-II airplane at moderate and low angles of attack in pushovers and straight flight at supersonic Mach numbers up to about 2.0 at altitudes between 50,000 and 70,000 feet. The paper presents some of the results of calculations of the dynamic lateral stability characteristics and also some results of the measurements of rudder hinge moments.

SYMBOLS

A_Y	lateral acceleration, g units
b	wing span, ft
C_{h_r}	rudder hinge-moment coefficient, $\frac{\text{Hinge moment}}{2qM_r}$
C_l	rolling-moment coefficient
C_n	yawing-moment coefficient
C_Y	lateral-force coefficient
C_N	airplane normal-force coefficient, Wn/qS
C_{l_β}	variation of rolling-moment coefficient with sideslip angle, $\partial C_l/\partial\beta$, per deg
C_{n_β}	variation of yawing-moment coefficient with sideslip angle, $\partial C_n/\partial\beta$, per deg

C_{Y_β} variation of side-force coefficient with sideslip angle, $\partial C_Y/\partial\beta$, per deg

C_{l_r} variation of rolling-moment coefficient with yawing-angular-velocity factor, $dC_l \Big/ d\frac{rb}{2V}$

C_{n_r} variation of yawing-moment coefficient with yawing-angular-velocity factor, $dC_n \Big/ d\frac{rb}{2V}$

C_{Y_r} variation of side-force coefficient with yawing-angular-velocity factor, $dC_Y \Big/ d\frac{rb}{2V}$

C_{l_p} variation of rolling-moment coefficient with rolling-angular-velocity factor, $dC_l \Big/ d\frac{pb}{2V}$

C_{n_p} variation of yawing-moment coefficient with rolling-angular-velocity factor, $dC_n \Big/ d\frac{pb}{2V}$

C_{Y_p} variation of side-force coefficient with rolling-angular-velocity factor, $dC_Y \Big/ d\frac{pb}{2V}$

$\bar{c}_r$ rudder mean aerodynamic chord, ft

g acceleration due to gravity, ft/sec^2

h_p pressure altitude, ft

I_X moment of inertia about longitudinal stability axis, $slug\text{-}ft^2$

I_Z moment of inertia about normal stability axis, $slug\text{-}ft^2$

M Mach number

M_r area moment of rudder about hinge line

n normal acceleration, g units

P	period, sec
p	rolling angular velocity, positive rolling to right, radians/sec
$\dot{p}$	rolling angular acceleration, radians/sec^2
p_e	nozzle exit pressure, lb/sq ft abs
p_0	static pressure, lb/sq ft abs
q	dynamic pressure, lb/sq ft
q_c'	uncorrected impact pressure, lb/sq ft
r	yawing angular velocity, positive yawing to right, radians/sec
S	wing area, sq ft
S_r	rudder area, sq ft
t	time, sec
$T_{1/2}$	time to damp to one-half amplitude, sec
V	true airspeed, ft/sec
W	airplane weight, lb
α	angle of attack of body center line, deg
β	angle of sideslip, positive when wind is from right, deg
δ_{a_L}	left aileron angle, positive for trailing edge down, deg
δ_r	rudder angle, positive when trailing edge is left, deg
δ_{a_T}	total aileron deflection, deg
γ	angle of flight path above horizontal, deg

ϵ angle of body axis relative to longitudinal principal axis of inertia, positive when body axis at nose is above principal axis, deg

η angle of longitudinal principal axis of inertia relative to flight path, positive when longitudinal principal axis above flight path at nose, deg

θ angle of fuselage reference line above horizontal, deg

φ roll angle, positive rolling to right, radians

INSTRUMENTATION AND METHODS

Standard NACA recording instruments were installed to measure the following pertinent quantities:

Airspeed and altitude
Aileron and rudder positions
Angles of attack and sideslip
Normal and transverse accelerations
Rolling and yawing angular velocities
Rudder hinge moment and rocket chamber pressure

All instruments were synchronized by a common timer.

The angles of attack and sideslip were measured from vanes mounted on the nose boom 42 and 37 inches, respectively, ahead of the apex of the airplane nose. No corrections were applied to the measured angles of attack and sideslip for upwash, sidewash, boom bending, pitching velocity, or yawing velocity inasmuch as the corrections would be negligible for the angles and rates encountered.

The rudder hinge moments were measured with strain gages on the rudder locking pin. This rudder locking device was located on the vertical tail adjacent to the inboard end of the rudder and slightly rearward of the rudder hinge line in the plane of symmetry. This position of the locking device did not completely preclude the possibility of rudder motion because of torsion due to aerodynamic loads. The torsional movement of the rudder in the locked position was small, however, compared to the movements experienced in the unlocked position.

The rudder control position transmitter was located on the side of the vertical tail at the rudder hinge line and in the plane of the bottom hinge of the rudder.

The roll position angles shown were obtained by integration of the rolling-velocity values.

The airspeed-altitude system was calibrated by comparing the static pressure measured in the airplane and the altitude of the airplane measured by radar with the pressure and altitude determined from a radiosonde balloon released at the time of each flight. In the supersonic range the accuracy of the position-error calibration is approximately $\Delta p/q_c' = 0.01$. This and other factors give a possible Mach number error of about ± 0.01 at $M = 1.0$ to about ± 0.04 at $M = 2.0$.

The airplane weight and center of gravity during flight were estimated from the known loaded and empty characteristics and the propellant consumption rate.

DESCRIPTION OF AIRPLANE

The airplane used in the present investigation has sweptback wing and tail surfaces and is equipped with plain flap-type unboosted control surfaces linked directly to the control wheel and rudder pedals. The airplane is powered by an LR8-RM-6 rocket engine which uses alcohol-water and liquid oxygen as propellants and has a design thrust of 6,000 pounds at sea level. Table I presents pertinent airplane physical characteristics and figure 1 is a three-view drawing. Shown in figure 2 is a photograph of the airplane.

For one of the flights the inboard fences, shown in figure 1, were installed on the airplane. Also during some of the flights the rocket engine was equipped with nozzle extensions designed to expand the exhaust gases to ambient pressure at an altitude of 28,000 feet. Figure 3 is a photograph of these nozzle extensions.

The inertia characteristics of the airplane are shown in table I. These values were based on the manufacturer's estimates. Figure 4 is a sketch showing the directions of the axes and angles pertinent to lateral stability measurements.

TESTS, RESULTS, AND DISCUSSION

Lateral Motions in Flight

During the early supersonic flights of the D-558-II, a reversal of rudder floating tendency with power on suggested the incorporation of a

lock to keep the rudder at zero, because it was felt that with lag or friction the apparent positive floating tendency may have been creating the objectionable lateral oscillation that occurred at the same time. (See ref. 2.) At a later time it was decided that, because the oscillation persisted, the pilot would be able to control the lateral motion better if he had the use of the rudder. As a consequence, data were obtained up to high Mach numbers with the rudder locked and unlocked.

The first flights to Mach numbers near 1.8 were performed by climbing the airplane to altitudes of about 55,000 feet and pushing over at nearly zero lift to a dive ($\alpha \approx -2^\circ$) with the rudder locked. During these flights, violent lateral oscillations occurred, with sideslip angles reaching $\pm 6^\circ$ and roll angles reaching about $\pm 60^\circ$. An example of one of these flights is shown in figure 5. It was decided that the low angle of attack, and consequent low inclination of the principal axis of inertia with respect to the flight path, may have aggravated the motion. A subsequent flight was made in which the pilot did not push over to low lift but maintained an angle of attack greater than 0°. In this condition, the lateral oscillation was much less pronounced. A time history of this flight is shown in figure 6. It should be noted that the two flights were made at different altitudes and at different constant angles of attack. Time histories of flights made with the rudder unlocked at both low and moderate angles of attack are shown in figures 7 and 8.

It will be noted that, in this paper, angles of attack below 0° are referred to as low and angles of attack between 0° and 5° are called moderate. This adopted convention of referring to the angles of attack may appear to be contrary to usual practice; however, it should be kept in mind that, although the angle of attack is relative to the fuselage center line, the wing has an incidence of 3°. Consequently, even though the fuselage may have a slight negative angle of attack, the wing itself will have a significant positive value.

Examination of the data presented in figures 5 to 8 shows that there is a large ratio of rolling to yawing with magnitudes between 6 and 8. This is probably primarily due to the large ratio of I_Z to I_X, to the rather low values of C_{l_p}, $(b/2V)$, high effective dihedral, and high altitude, all of which tend to create poor dynamic lateral stability characteristics.

By using data from the flights of figures 5 to 8 and other flights, plots were made of the variation of the amplitude of the sideslip oscillation with angle of attack, for both the rudder-locked and rudder-unlocked conditions while the pilot was attempting to control the motion (fig. 9). The original data from which these curves of figure 9 were made covered a wide range of sideslip amplitude at any angle of attack. However, the

curves shown represent the lower limit to which the pilot could keep the motion and are shown in order to give a qualitative indication of the effects of angle of attack and of locking the rudder on the ability of a pilot to control the lateral motions of the airplane. Figure 9 shows that this lower limit of sideslip amplitude was much greater at the lower angles of attack at all Mach numbers and also increased with increasing Mach number. It should be pointed out that, at all speeds in any flight conditions, there was almost always a small residual oscillation; however, except for the conditions shown here, the amplitude of these oscillations could be kept to nearly zero by concerted effort by the pilot. It is apparent from figure 8 that the pilot could control the motion more easily when he was able to use coordinated aileron and rudder controls. The pilot's ability to control the motion was not affected materially by the positive rudder floating tendency caused by power, and the airplane motion could be lead sufficiently to keep the amplitude lower than with the rudder locked. A later section of this paper describes the rudder hinge moments measured during these flights.

It has been proposed that perhaps power will have a noticeable effect on the lateral airplane characteristics by changing the flow at the tail. As yet there is no evidence from flight data to indicate that there is an appreciable effect of power on the overall stability characteristics of the airplane, and the wind-tunnel data of reference 3 indicate that the effect of power on the rudder-fixed contribution of the vertical tail is negligible.

The experience gained from these earlier flights enabled the pilot to fly the airplane at still higher Mach numbers by flying at an angle of attack high enough so that he was able to control the lateral motions. Data obtained during a flight to a Mach number of 2.0 are shown in figure 10. It should be noted that the pilot increased the angle of attack at the higher Mach numbers.

During one of the flights with the rudder locked, the pilot attempted to hold the ailerons fixed for a period of time in order to determine the lateral motion that would ensue (see fig. 11, time 50 to 55.5 seconds). The airplane tended to roll off at a fairly rapid rate until the roll angle reached about 90°, at which time the pilot stopped the motion with the ailerons. During another flight at a low angle of attack with the rudder locked, previously shown in figure 5, the lateral motion was of such a nature that the airplane rolled nearly 140° although the pilot was trying to control the airplane with the ailerons. At one time during the flight when the pilot felt that the controls were ineffective in stopping the rolling motion (fig. 5, time 42 seconds) the pilot reversed the aileron controls in order to make the airplane complete the roll to 360° in order to recover from the inverted attitude. This action was also ineffective as the airplane at the same time apparently began to recover

of its own accord against the control motion supplied by the pilot. It is pertinent to point out here that this condition was not caused by a complete lack of aileron effectiveness. Unpublished flight data indicate that aileron effectiveness at these speeds is indeed low but that an appreciable amount of aileron effectiveness still remains. At an altitude of 60,000 feet and a Mach number of approximately 1.9, $\frac{\partial\left(\frac{pb}{2V}\right)}{\partial\delta_{a_T}}$ is in the vicinity of 0.0007.

The motions obtained during these two flights suggest the possibility that the control-fixed transient oscillation at high supersonic speeds at low angles of attack may be one in which the roll angles reach values in excess of 90°, whereas the transient sideslip angles remain at relatively low values. However, because of the difficulty of flying the airplane at these speeds and angles of attack, it has not been possible to check this hypothesis further in flight.

Results of Calculations of Period and Damping

In order to obtain some indication of the actual importance of the changes of flight conditions on the control-fixed dynamic stability characteristics, calculations of period and damping were made. The static derivatives used in the calculations are shown in figure 12 and were obtained by fairing the wind-tunnel data of references 3 and 4. Although static-derivative data from reference 5 for a Mach number of 2.01 are shown in figure 12, these data were not employed in the fairing because of the very large value of C_{l_β} and the lack of data in reference 5 at other Mach numbers. Admittedly the fairings may be somewhat low; however, in the present report this is not believed to be critical since the calculations were made to show the qualitative influence of changes in inclination of the principal axis. It should be noted that the vertical tail on the wind-tunnel model of reference 4 was somewhat smaller than that used on the airplane and on the model of reference 3. The ratio of the vertical-tail area of reference 4 to that of reference 3 is 1.06. The ratio of areas is based on areas bounded by the leading and trailing edges, the tip, and the line drawn from the intersection of the leading edge (disregarding dorsal fin) and the fuselage parallel to the center line of the fuselage. The actual areas of the large and small tails on the basis of the prototype airplane are 36.6 and 32.2 square feet, respectively.

The yawing and rolling derivatives were calculated by determining, from references 3 and 4, the tail contribution to C_{Y_β}, utilizing the mathematical relations for evaluating the tail contributions to the

rolling derivatives and yawing derivatives as presented in references 6 and 7, respectively, and adding to the tail contributions the wing contributions to the rolling derivatives as calculated from references 8 and 9 and the wing contributions to the yawing derivative C_{l_r} as calculated from reference 9. The wing contributions to C_{Y_r} and C_{n_r} were considered to be negligible.

With these derivatives and the mass characteristics given in table I, the inverse of the time to damp to one-half amplitude and the period of the lateral motions in level flight were computed for a range of Mach number from 1.6 to 2.2 for altitudes of 60,000 and 75,000 feet. The results of these calculations are presented in figure 13. The negative values of the inverse of the time to damp to one-half amplitude signify the inverse of the time to double the amplitude. Because of the uncertainty of the mass characteristics, the computations were made for angles of principal-axis inclination of 2° and 3°. Figure 13 shows that both an arbitrary change in principal-axis inclination of 1° and the change in principal-axis location resulting from a change in angle of attack required to fly at different altitudes have appreciable effects on the damping of the lateral motion and also that at the higher speeds the deterioration of the stability derivatives creates a reduction of dynamic stability as the Mach number increases. The time histories of figures 5 to 8 and 10 appear to have oscillations with periods much greater than the calculations indicate. It is important to note that in attempting to damp the motions of the airplane, the pilot was using controls during the flights shown in figures 6 and 7; it appears that these attempts to damp the motions of the airplane generally tended to increase the period of the oscillations. Also, the calculations assume small disturbance, and the displacements in roll, at least, were not small by any means. When rolling angles of the magnitude of $\pm 90^\circ$ are present, the small-displacement theory is not applicable to the adequate prediction of lateral oscillatory characteristics.

Rudder Hinge Moments

The rudder hinge moments were measured during sideslip oscillations with the rudder locked. During most of these oscillations, the rolling was violent and, because of this and sidewash, the sideslip angles measured at the nose of the airplane may be very different from the true sideslip at the tail. In figure 14 are shown typical variations of rudder hinge-moment coefficient with sideslip angle, power off and power on (original nozzles).

Figure 14 shows that the variation of hinge-moment coefficient with sideslip angle is not rectilinear, that the power-off variation of C_{h_r}

with β becomes steeper at larger sideslip angles, and that the power-on variation of C_{h_r} with β appears to reverse at larger sideslip angles; these results thus indicate that the positive floating tendency of the rudder exists only for small sideslip angles. Reference 3 also indicates that the positive floating tendency with high pressure ratios exists only at small sideslip angles.

The variation of the hinge-moment parameter $dC_{h_r}/d\beta$ with Mach number and pressure ratio is shown in figure 15. These data were obtained with power off $(p_e/p_0 = 0)$, with original nozzles $(p_e/p_0 = 8 \text{ to } 16)$, and with nozzle extensions $(p_e/p_0 = 2 \text{ to } 7)$. The slopes in figure 15 were taken at small sideslip angles and give only an indication of the hinge moments in this region of small sideslip angles. There was considerable scatter in the data at any Mach number and pressure ratio, sometimes as much as ± 20 percent of the indicated value of $dC_{h_r}/d\beta$ at the higher values, and the curves presented should only be considered as a qualitative indication of the effects of Mach number and pressure ratio on hinge moments. These figures show that with empennage installations such as those of the D-558-II, the floating tendency of a control surface may tend to become positive at small angles of attack or sideslip and that, at high pressure ratios, the positive floating tendency may be very strong. The results of erratic hinge moments can be disturbing to a pilot using a reversible control system.

SUMMARY OF RESULTS

Flight tests, wind-tunnel data, and calculations of the lateral stability characteristics of the D-558-II airplane to Mach numbers of 2.0 indicate the following results:

1. At an angle of attack of -2°, the airplane experienced violent lateral motions through the supersonic speed range and roll angles reached $\pm 60^\circ$.

2. A positive increase of the inclination of the principal axis with respect to the flight path resulting from the increased angle of attack greatly improved the dynamic lateral characteristics.

3. The dynamic lateral stability decreased with increasing Mach number, apparently as a result of a deterioration of some of the important stability derivatives with increasing Mach number in the supersonic region of flight.

4. High ratios of rocket-exhaust pressure to static pressure created large changes in rudder hinge-moment characteristics; however, the effect of power on the overall lateral handling qualities appears to be negligible.

High-Speed Flight Station,
National Advisory Committee for Aeronautics,
Edwards, Calif., September 22, 1954

REFERENCES

1. Sjoberg, Sigurd A.: Preliminary Measurements of the Dynamic Lateral Stability Characteristics of the Douglas D-558-II (BuAero No. 37974) Airplane. NACA RM L9G18, 1949.

2. Ankenbruck, Herman O., and Dahlen, Theodore E.: Some Measurements of Flying Qualities of a Douglas D-558-II Research Airplane During Flights to Supersonic Speeds. NACA RM L53A06, 1953.

3. Grigsby, Carl E.: An Investigation of the Effects of Jet Exhaust and Reynolds Number Upon the Flow Over the Vertical Stabilizer and Rudder of the Douglas D-558-II Research Airplane at Mach Numbers of 1.62, 1.93, and 2.41. NACA RM L54E03, 1954.

4. Grant, Frederick C., and Robinson, Ross B.: Static Lateral Stability Characteristics of a 1/16-Scale Model of the Douglas D-558-II Research Airplane at Mach Numbers of 1.61 and 2.01. NACA RM L53I29a, 1953.

5. Robinson, Ross B.: Effects of Canopy, Revised Vertical Tail, and a Yaw-Damper Vane on the Aerodynamic Characteristics of a 1/16-Scale Model of the Douglas D-558-II Research Airplane at a Mach Number of 2.01. NACA RM L54F25, 1954.

6. Letko, William, and Riley, Donald R.: Effect of an Unswept Wing on the Contribution of Unswept-Tail Configurations to the Low-Speed Static- and Rolling-Stability Derivatives of a Midwing Airplane Model. NACA TN 2175, 1950.

7. McNeill, Walter E., and Cooper, George E.: A Comparison of the Measured and Predicted Lateral Oscillatory Characteristics of a 35° Swept-Wing Fighter Airplane. NACA RM A51C28, 1951.

8. Harmon, Sidney M., and Martin, John C.: Theoretical Calculations of the Lateral Force and Yawing Moment Due to Rolling at Supersonic Speeds for Sweptback Tapered Wings With Streamwise Tips. Supersonic Leading Edges. NACA TN 2156, 1950.

9. Jones, Arthur L., and Alksne, Alberta: A Summary of Lateral-Stability Derivatives Calculated for Wing Plan Forms in Supersonic Flow. NACA Rep. 1052, 1951.

TABLE I

PHYSICAL CHARACTERISTICS OF THE DOUGLAS D-558-II AIRPLANE

Wing:	
Root airfoil section (normal to 0.30 chord of unswept panel)	NACA 63-010
Tip airfoil section (normal to 0.30 chord of unswept panel)	NACA 63_1-012
Total area, sq ft	175.0
Span, ft	25.0
Mean aerodynamic chord, in.	87.301
Root chord (parallel to plane of symmetry), in.	108.51
Extended tip chord (parallel to plane of symmetry), in.	61.18
Taper ratio	0.565
Aspect ratio	3.570
Sweep at 0.30 chord of unswept panel, deg	35.0
Sweep of leading edge, deg	38.8
Incidence at fuselage center line, deg	3.0
Dihedral, deg	-3.0
Geometric twist, deg	0
Total aileron area (rearward of hinge line), sq ft	9.8
Aileron travel (each), deg	±15
Total flap area, sq ft	12.58
Flap travel, deg	50
Horizontal tail:	
Root airfoil section (normal to 0.30 chord of unswept panel)	NACA 63-010
Tip airfoil section (normal to 0.30 chord of unswept panel)	NACA 63-010
Total area, sq ft	39.9
Span, in.	143.6
Mean aerodynamic chord, in.	41.75
Root chord (parallel to plane of symmetry), in.	53.6
Extended tip chord (parallel to plane of symmetry), in.	26.8
Taper ratio	0.50
Aspect ratio	3.59
Sweep at 0.30 chord line of unswept panel, deg	40.0
Dihedral, deg	0
Elevator area, sq ft	9.4
Elevator travel, deg	
Up	25
Down	15
Stabilizer travel, deg	
Leading edge up	4
Leading edge down	5

TABLE I - Concluded

PHYSICAL CHARACTERISTICS OF THE DOUGLAS D-558-II AIRPLANE

Vertical tail:	
Airfoil section (normal to 0.30 chord of unswept panel)	NACA 63-010
Effective area (area above root chord), sq ft	36.6
Height from fuselage reference line, in.	98.0
Root chord (chord 24 in. above fuselage reference line), in.	116.8
Extended tip chord (parallel to fuselage reference line), in.	27.0
Sweep angle at 0.30 chord of unswept panel, deg	49.0
Rudder area (aft hinge line), sq ft	6.15
Rudder travel, deg	±25
Rudder mean aerodynamic chord, in.	15.27
Fuselage:	
Length, ft	42.0
Maximum diameter, in.	60.0
Fineness ratio	8.40
Speed-retarder area, sq ft	5.25
Power plane:	
Rocket	LR8-RM-6
Airplane weight, lb:	
Full rocket fuel	15,787
No fuel	9,421
Center-of-gravity locations, percent M.A.C.:	
Full rocket fuel (gear up)	24.6
No fuel (gear up)	27.3
No fuel (gear down)	26.7
Moments of inertia (no fuel), slug-ft^2:	
About normal principal axis	32,000
About longitudinal principal axis	2,900
About lateral axis	30,500

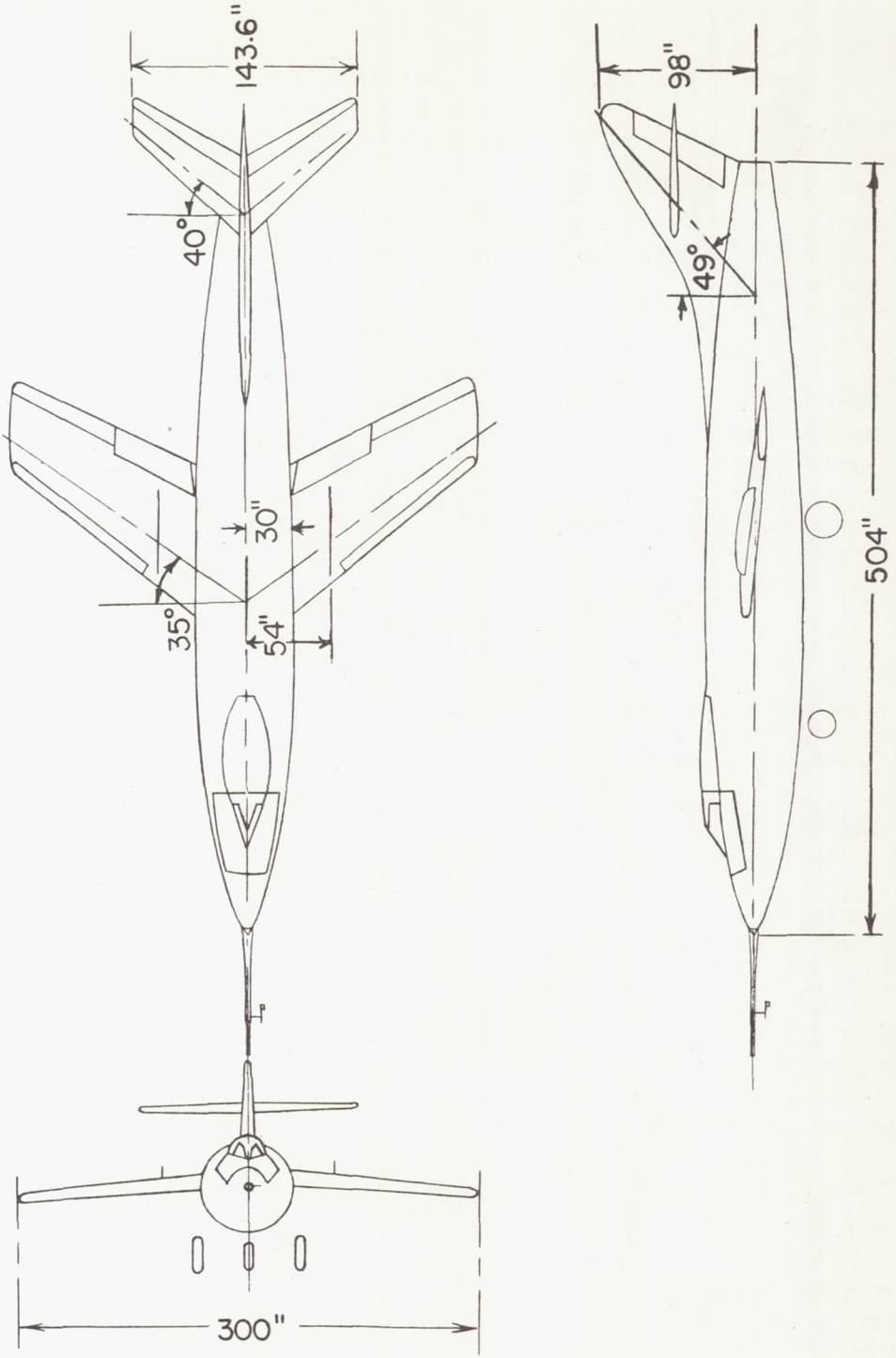

Figure 1.- Three-view drawing of the Douglas D-558-II research airplane. All dimensions are in inches.

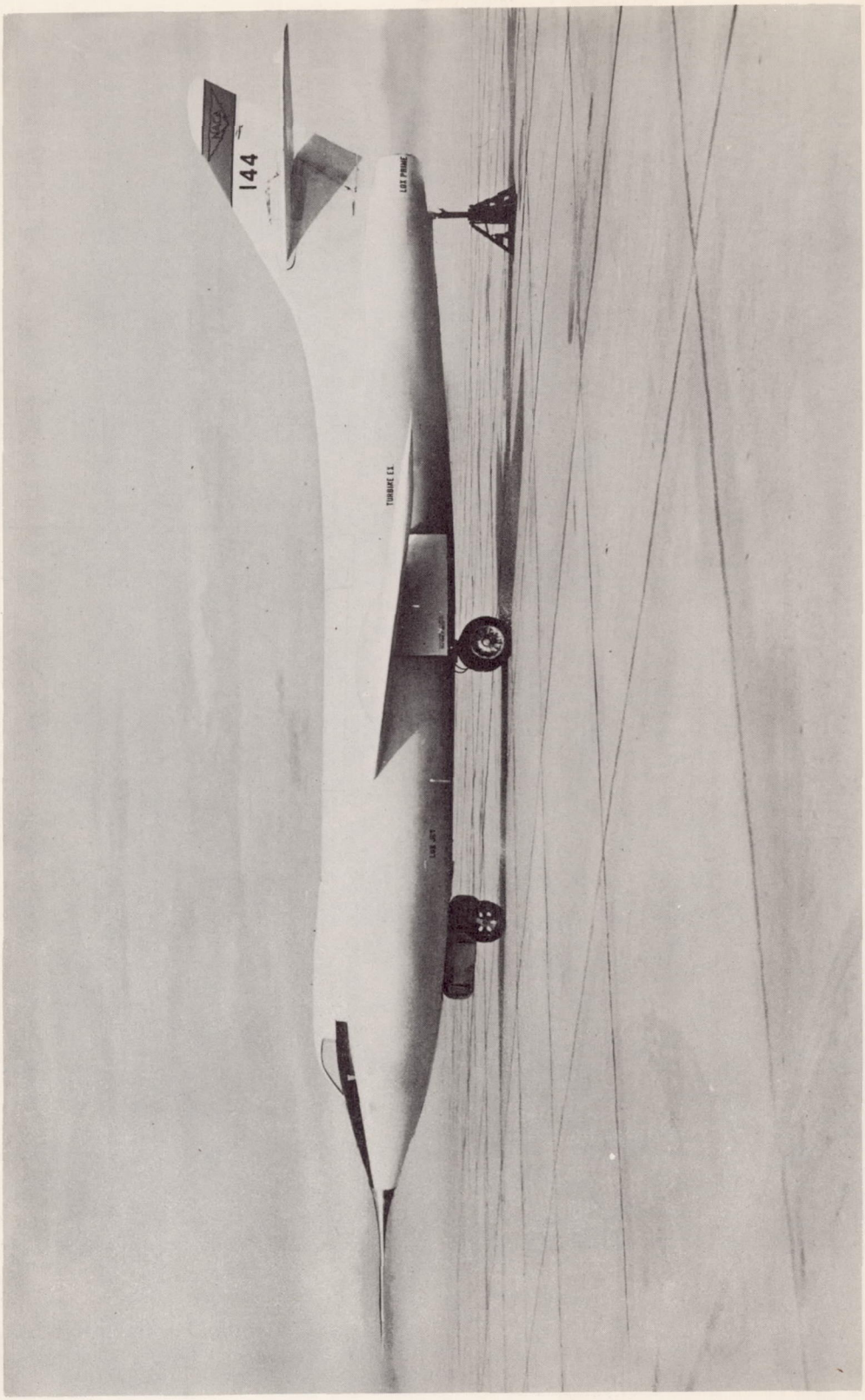

L-73284

Figure 2.- Side view of the Douglas D-558-II all-rocket research airplane.

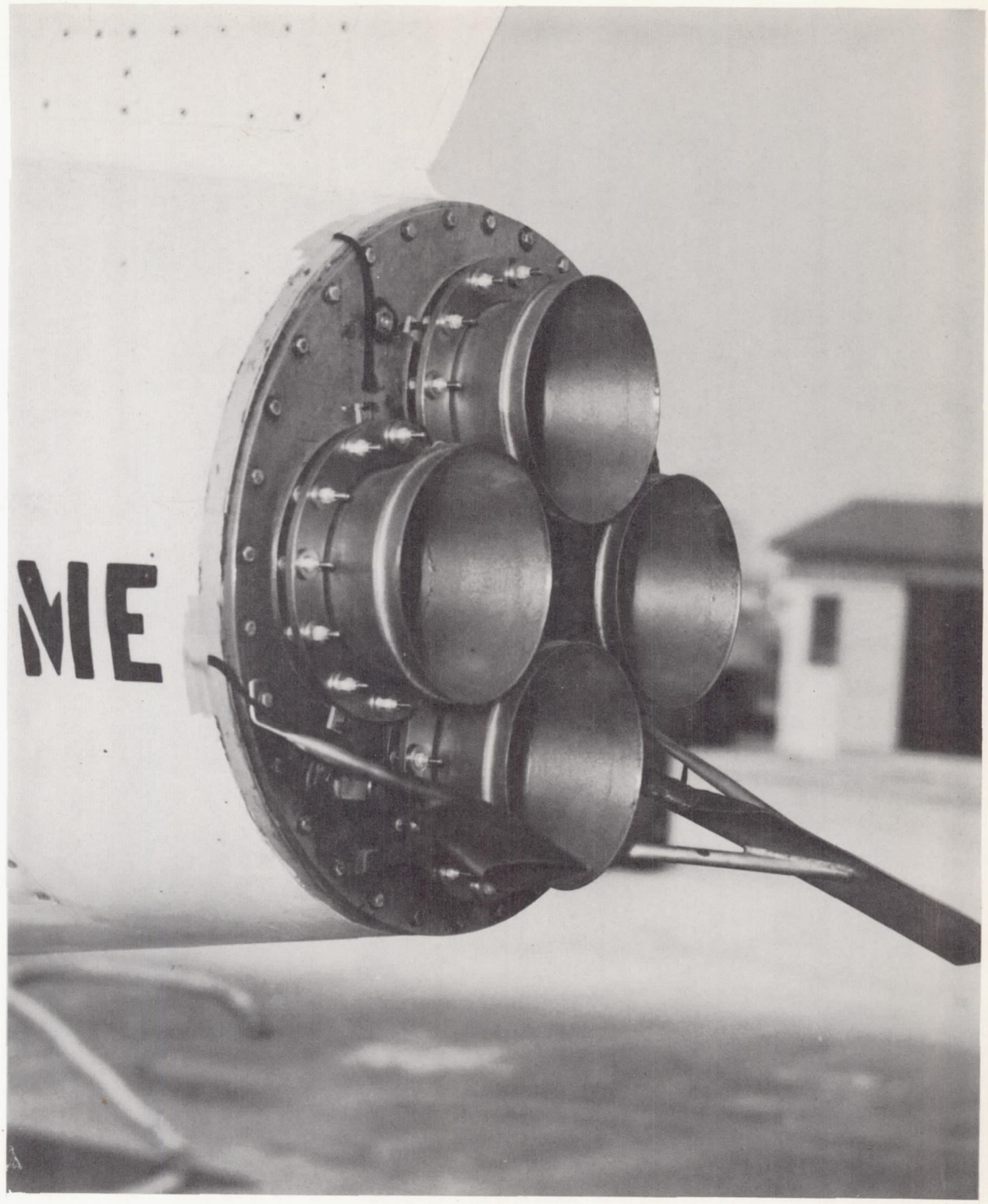

L-85678

Figure 3.- Nozzle extensions on the Douglas D-558-II all-rocket research airplane.

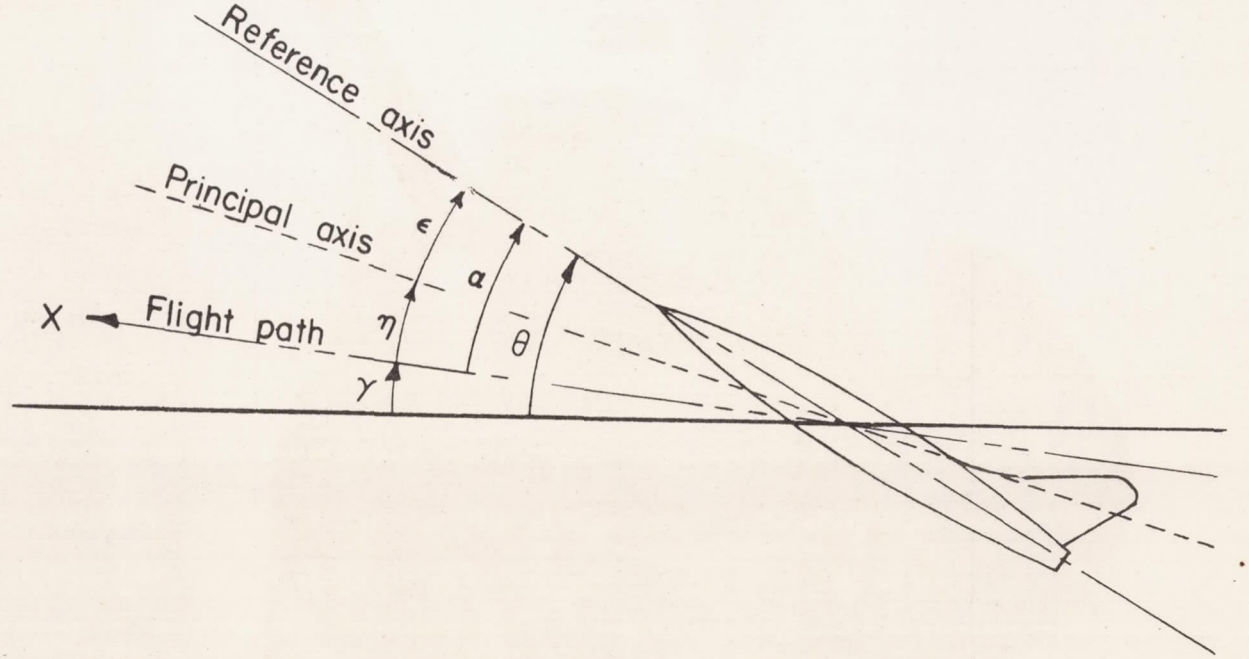

Figure 4.- System of axes and angular relationships in flight. Arrows indicate positive direction of angles. $\alpha = \eta + \epsilon$.

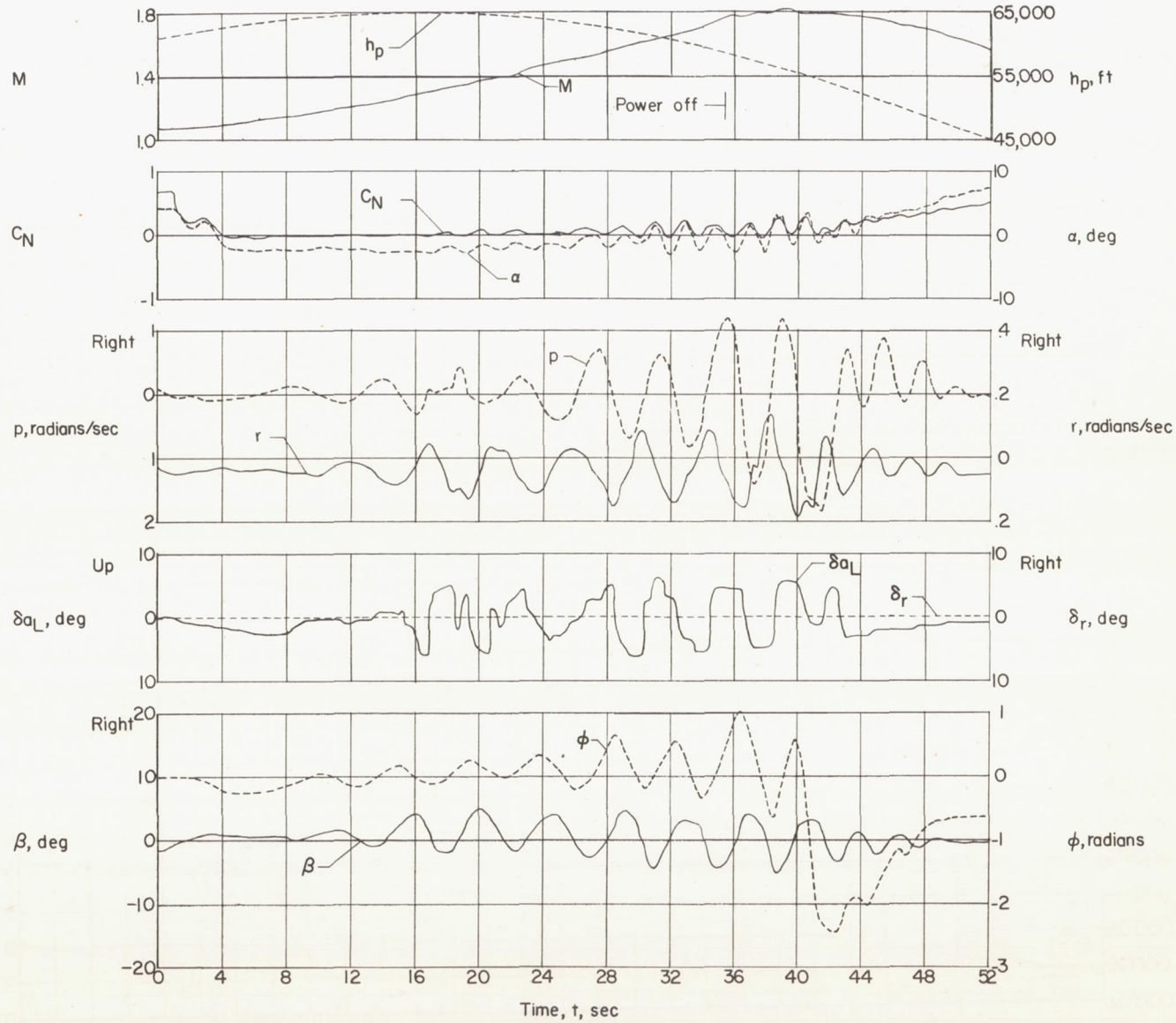

Figure 5.- Time history of data obtained during a pushover and dive at low angle of attack. Rudder locked.

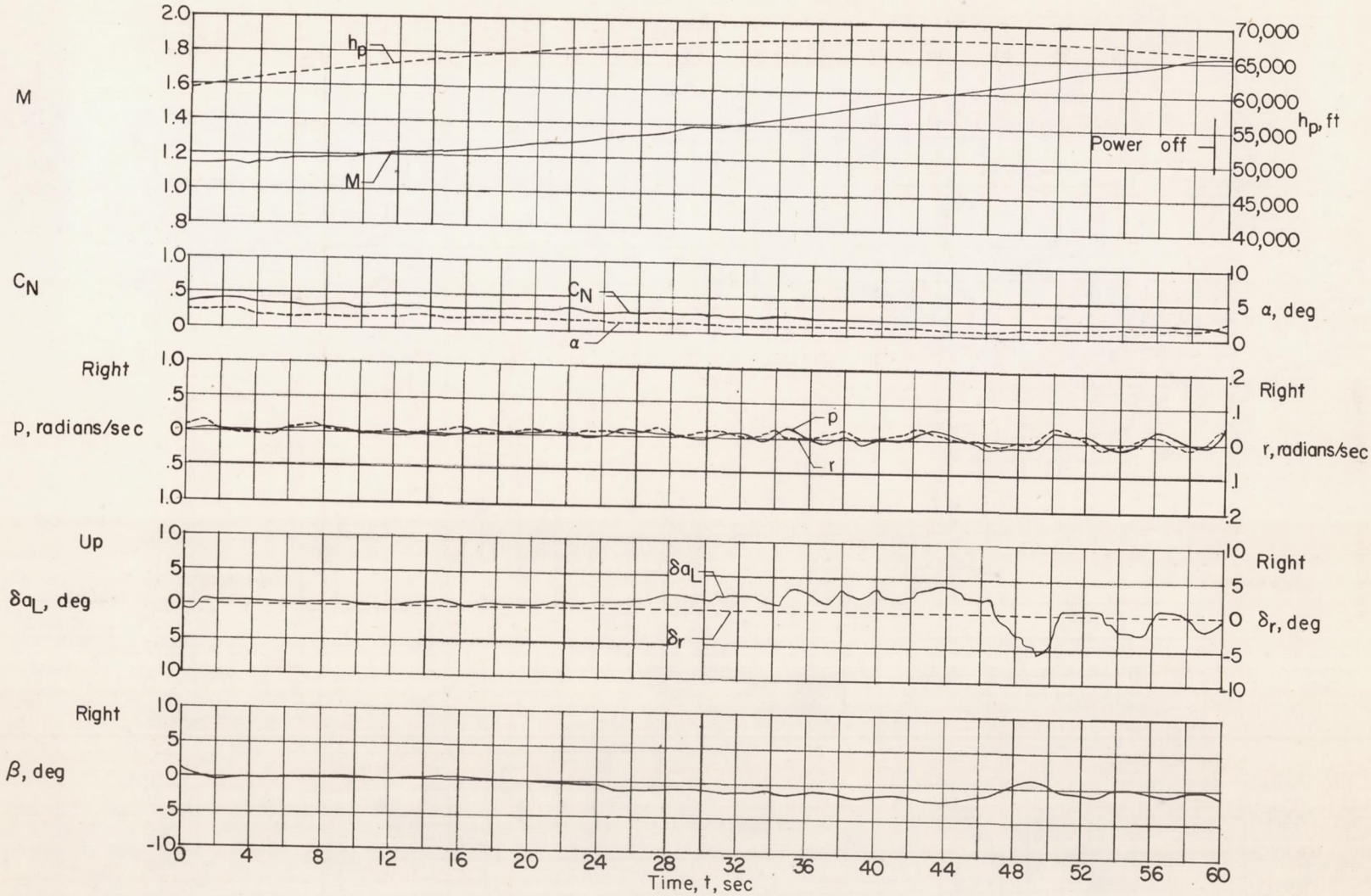

Figure 6.- Time history of data obtained during a straight flight at moderate angle of attack. Rudder locked.

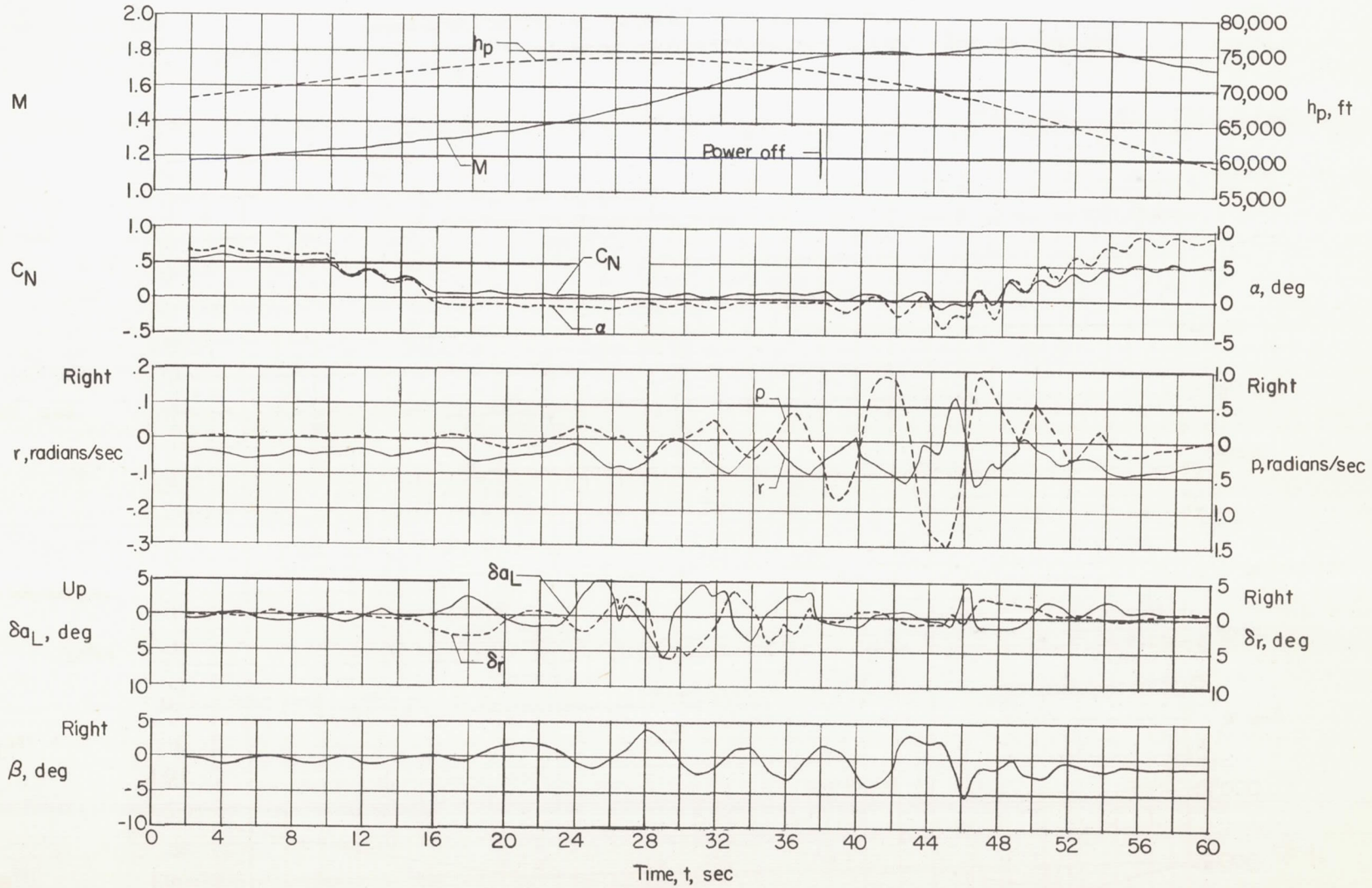

Figure 7.- Time history of data obtained during a pushover and dive at low angle of attack. Rudder unlocked.

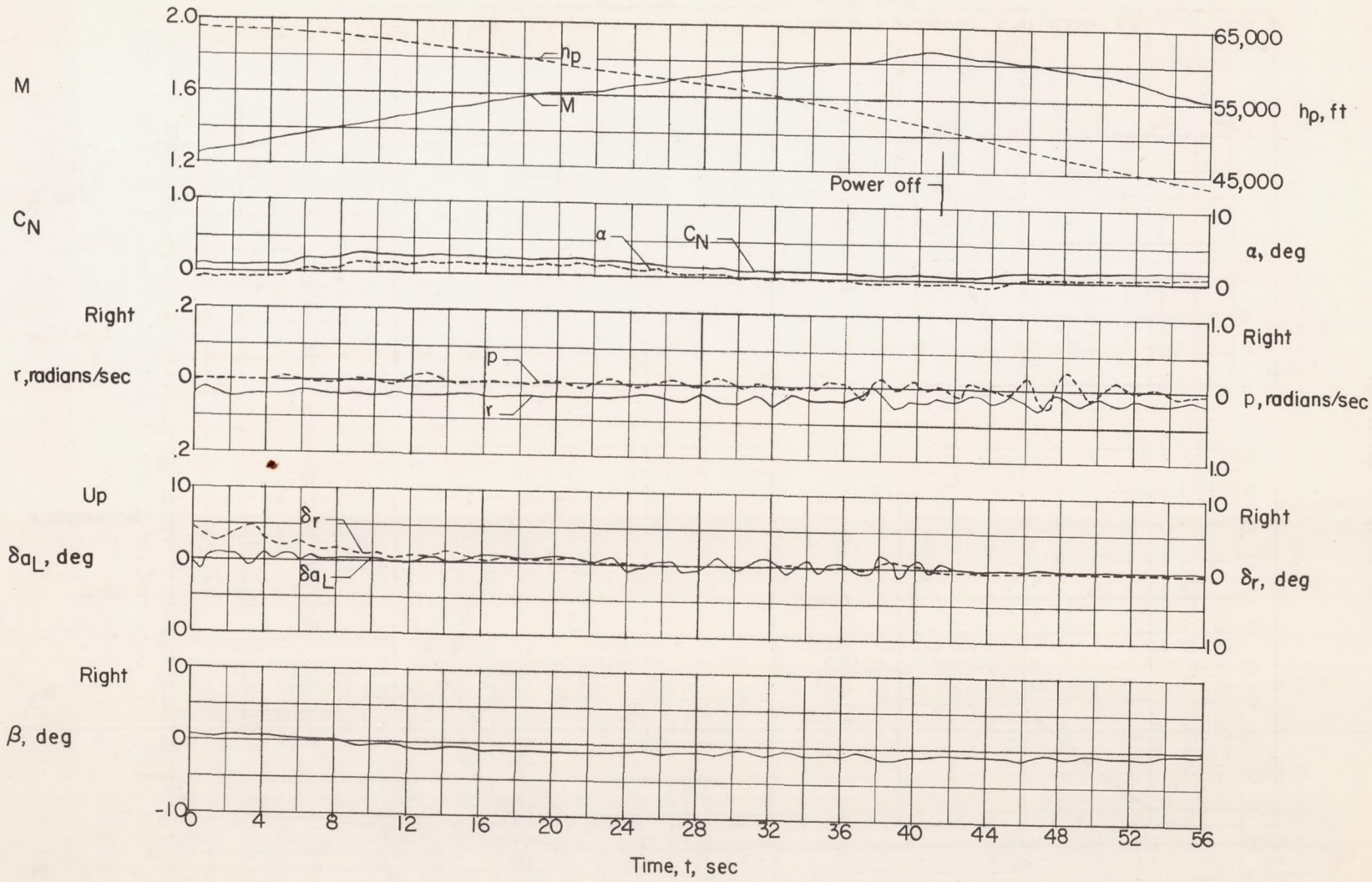

Figure 8.- Time history of data obtained during a straight flight at moderate angle of attack. Rudder unlocked.

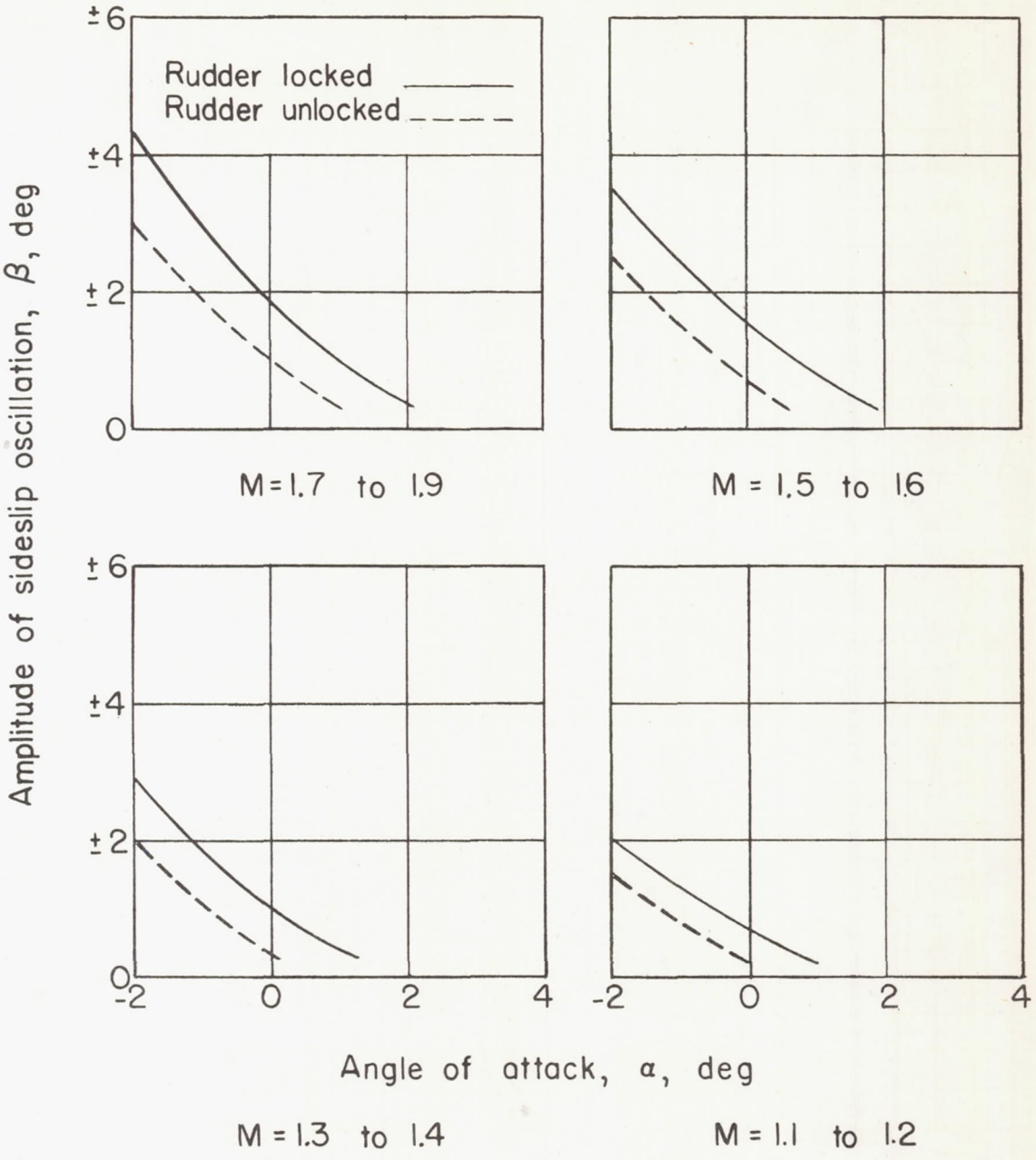

Figure 9.- Approximate variation with angle of attack and Mach number of minimum sideslip amplitudes to which the pilot could control the sideslip motions.

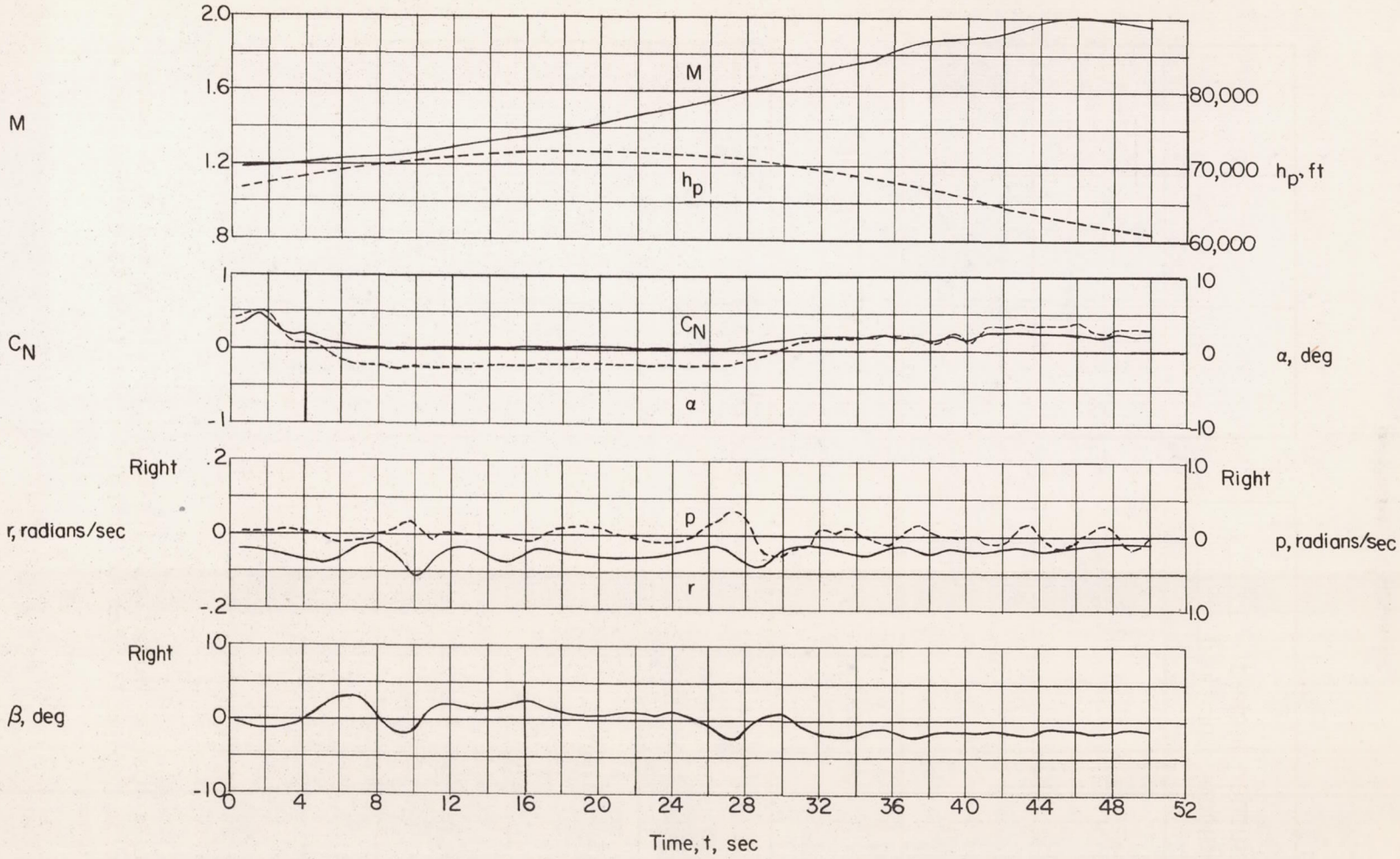

Figure 10.- Time history of data obtained during a flight to a Mach number of 2.0. Rudder unlocked. Rudder and aileron positions not available.

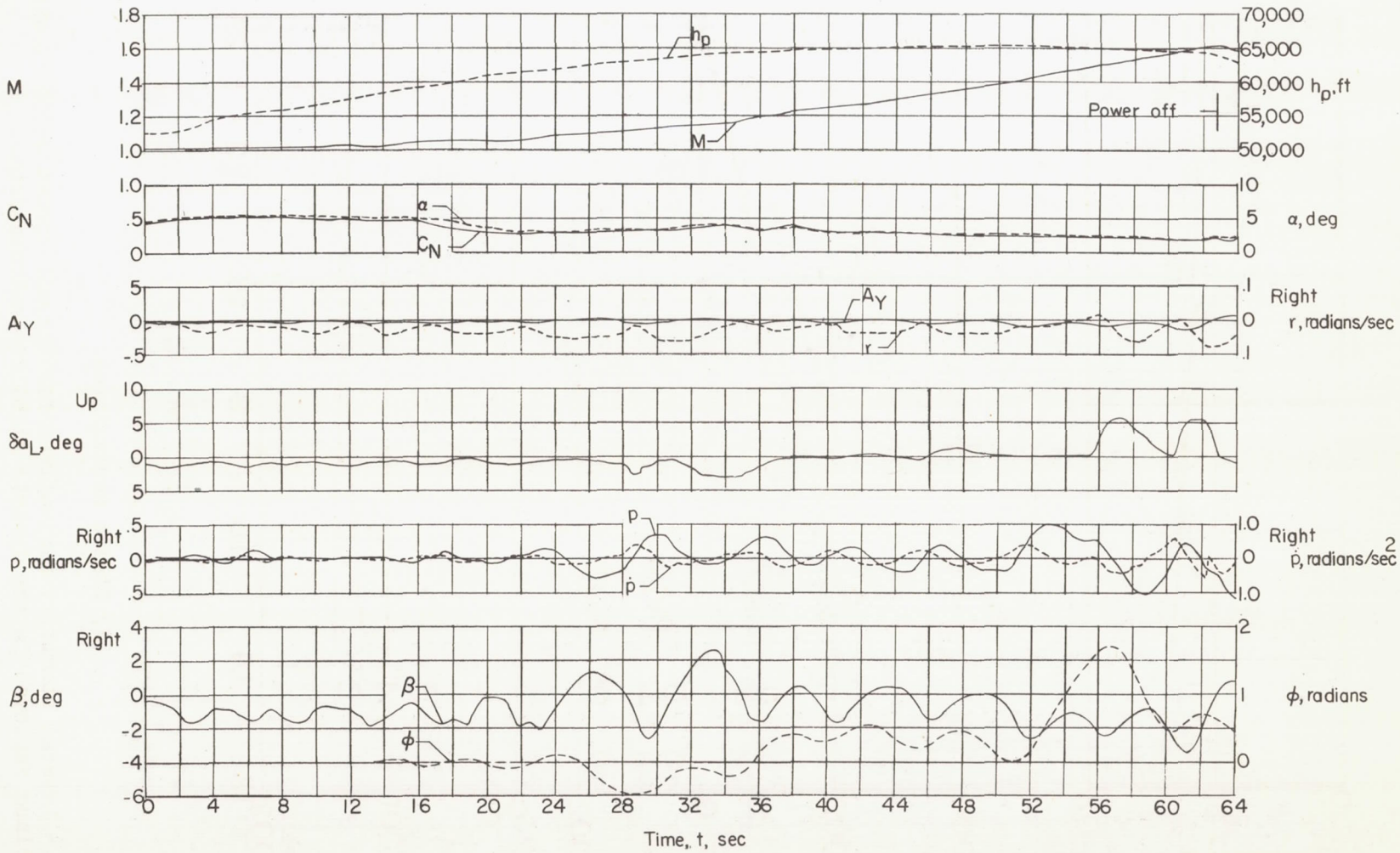

Figure 11.- Time history of data obtained during a straight flight at moderate angle of attack, rudder locked, during which the pilot held ailerons fixed for a period of time. Inboard fences on.

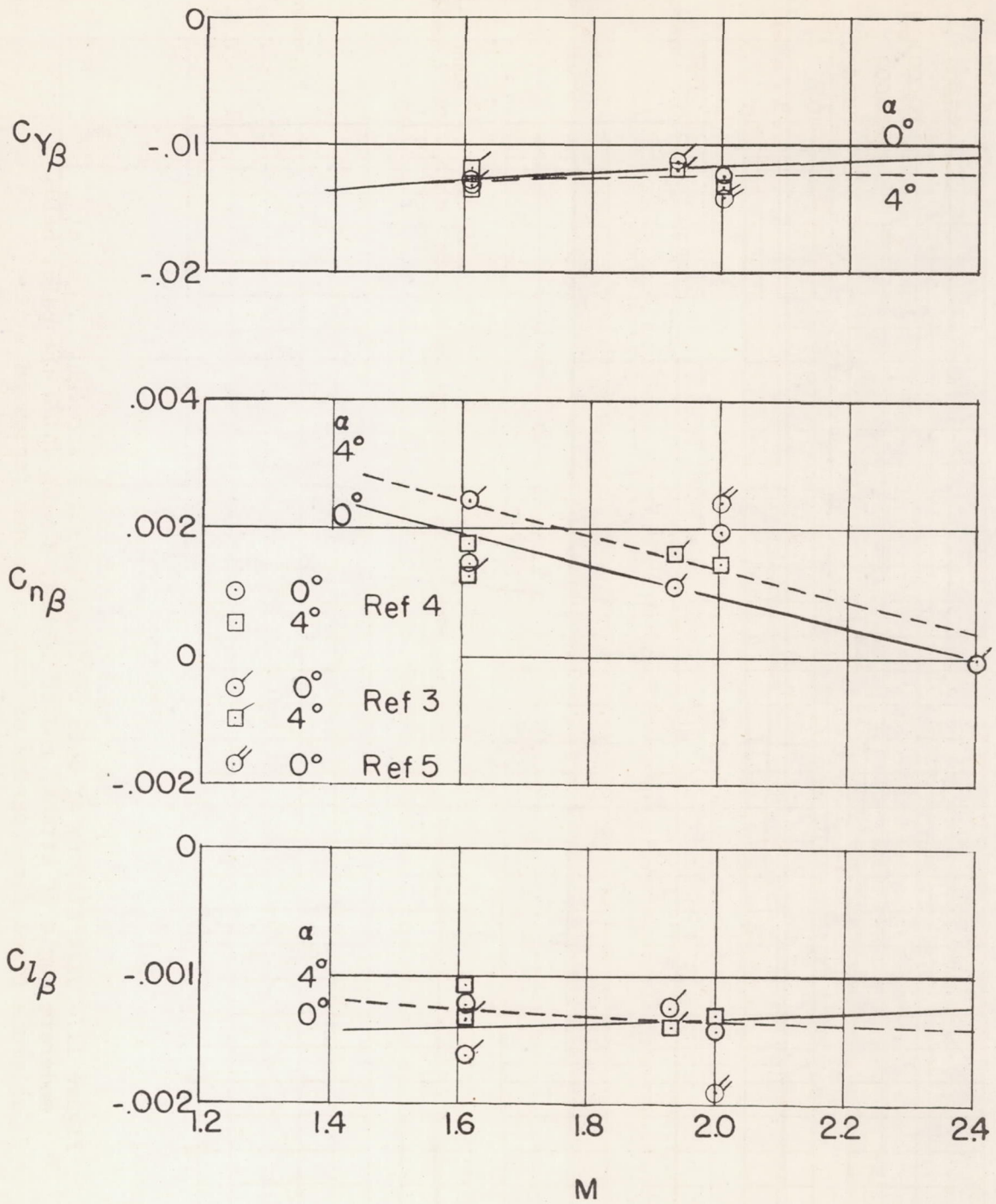

(a) Static derivatives.

Figure 12.- Lateral stability derivatives for the all-rocket D-558-II airplane employed in the dynamic stability calculations.

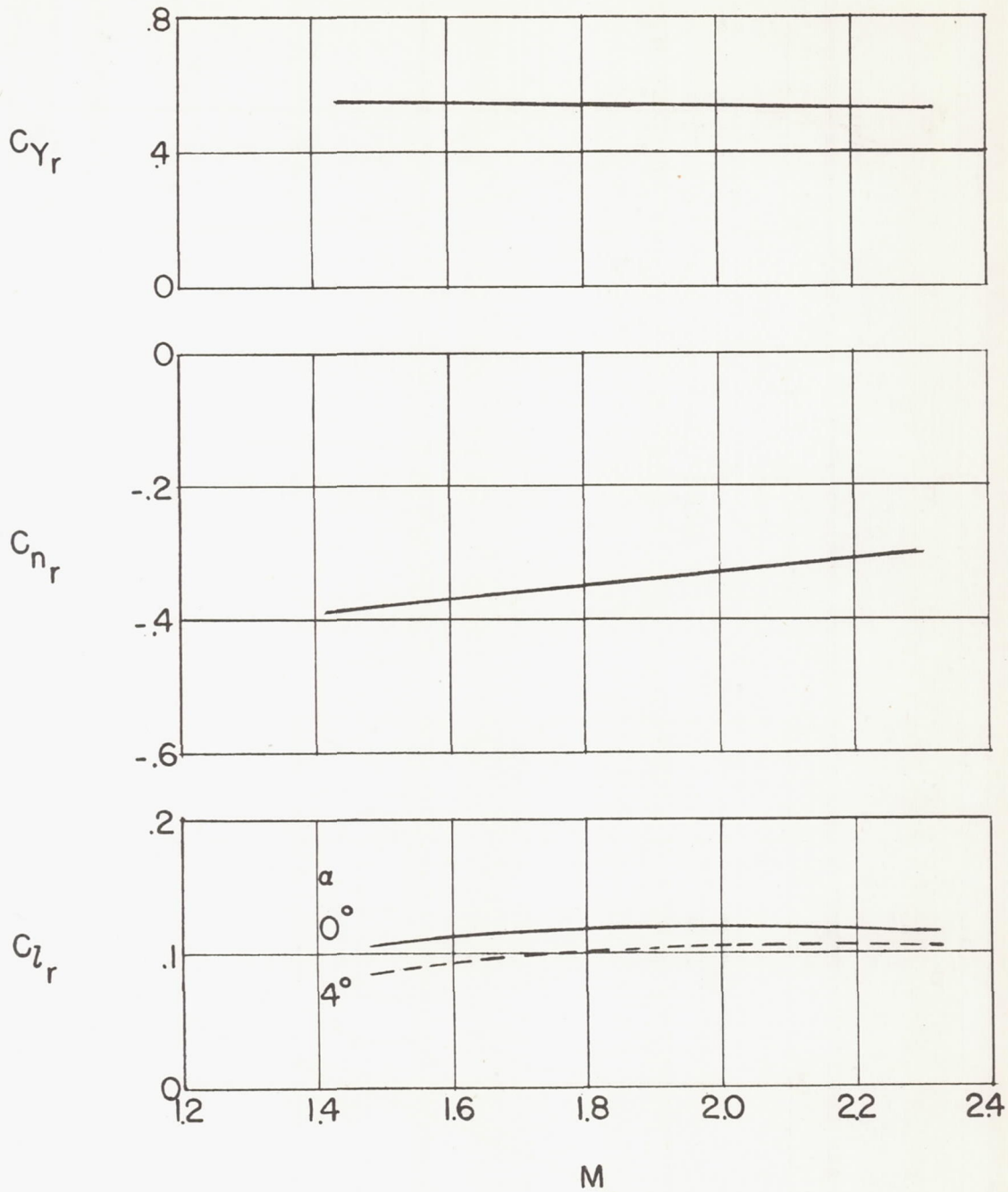

(b) Yawing derivatives.

Figure 12.- Continued.

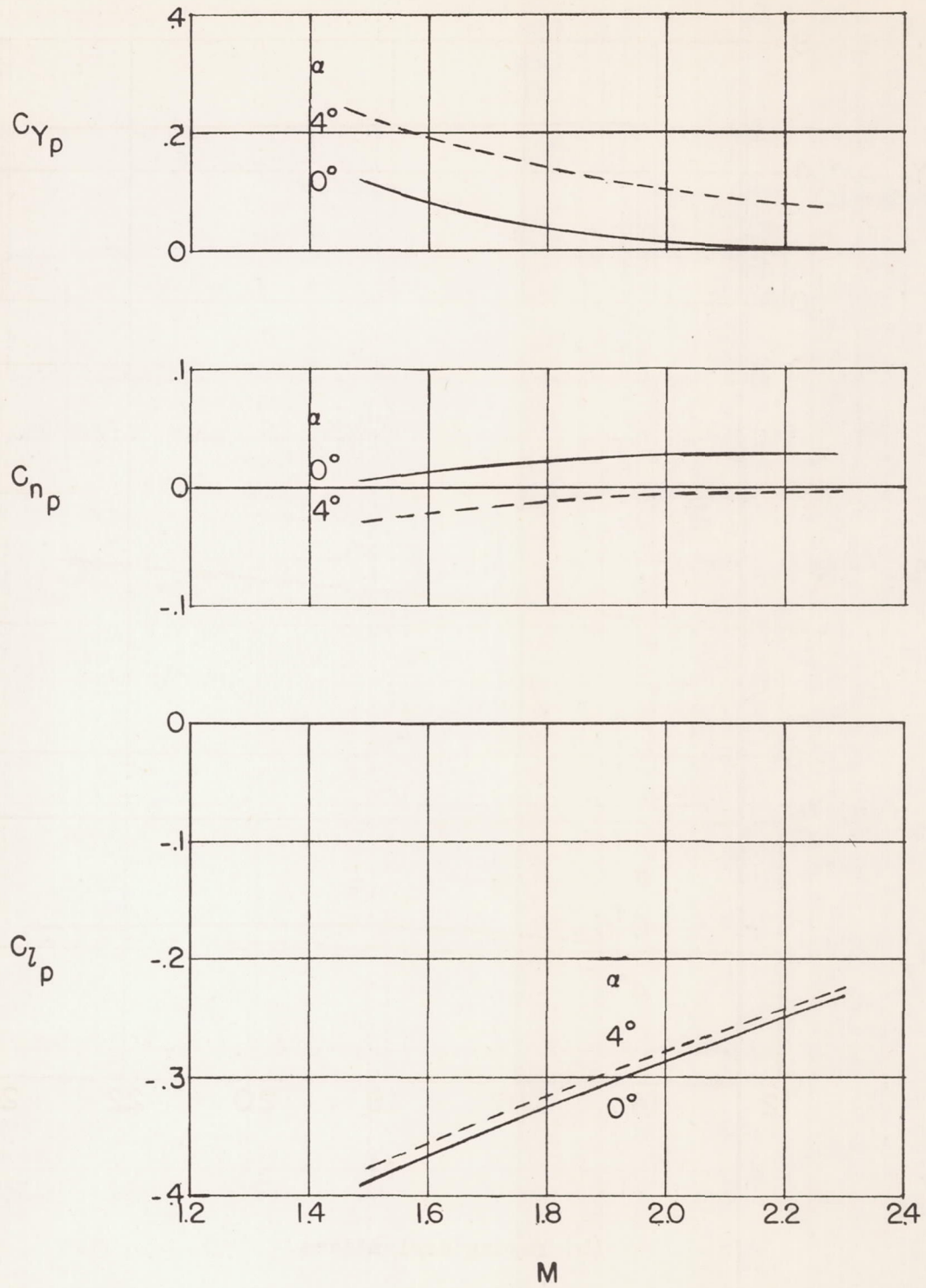

(c) Rolling derivatives.

Figure 12.- Concluded.

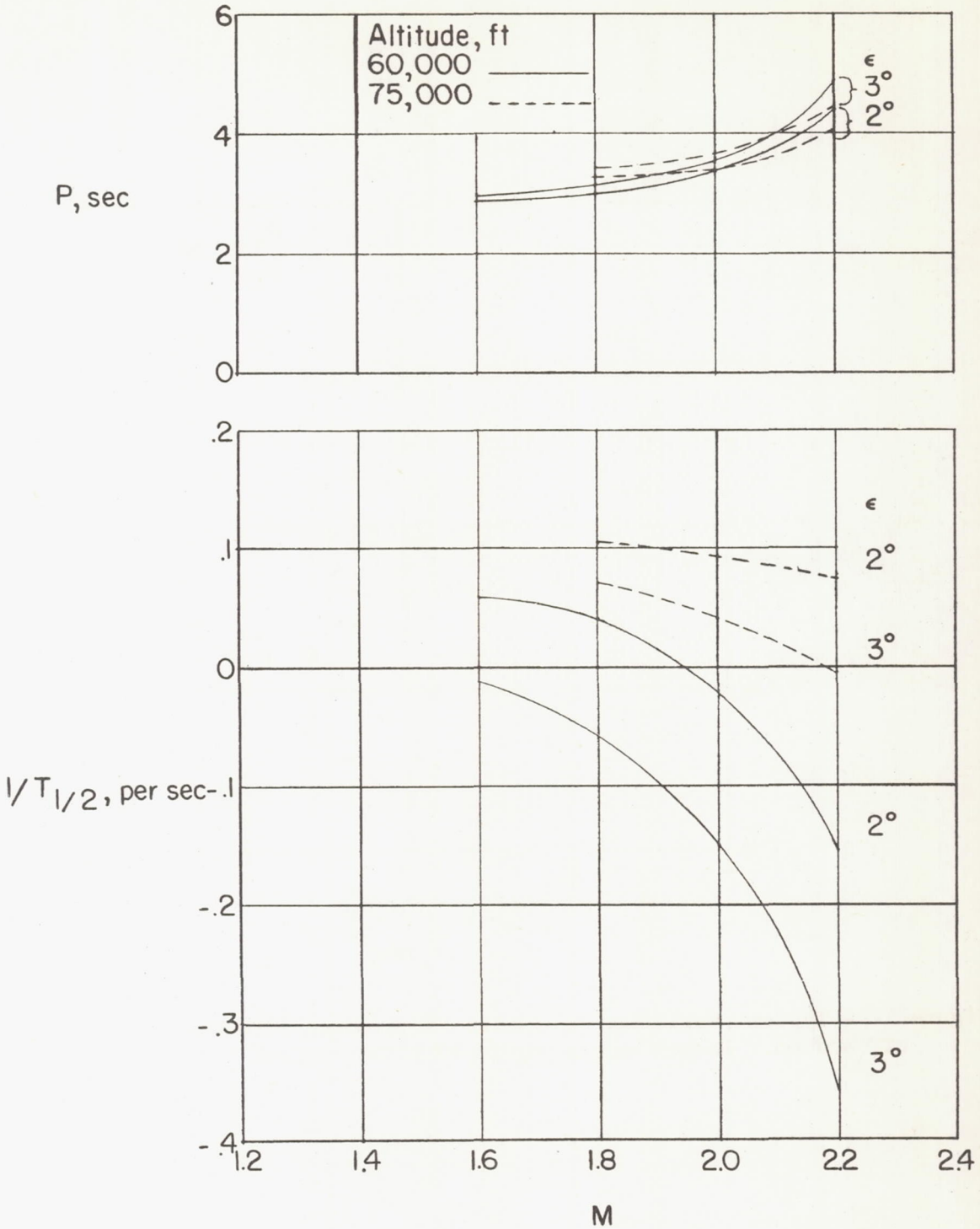

Figure 13.- Calculated period and damping for principal-axis inclination of 2° and 3°.

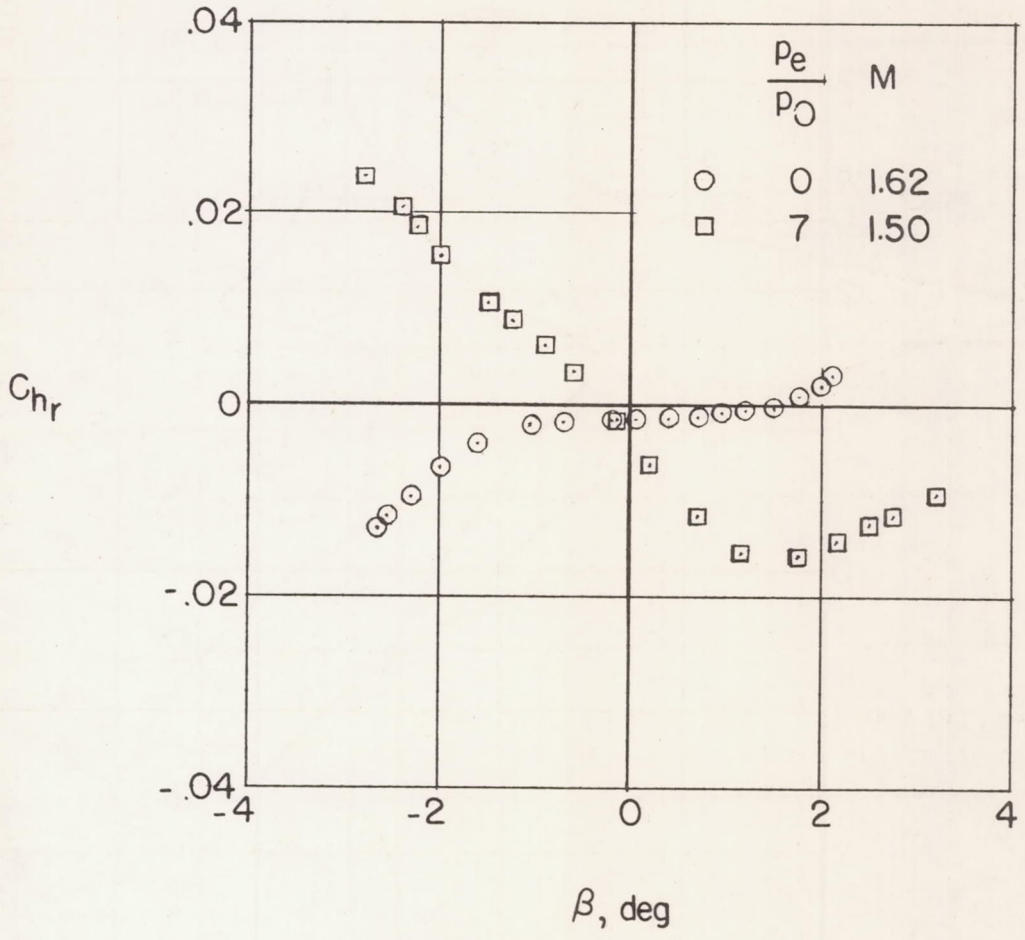

Figure 14.- Typical variation of rudder hinge-moment coefficient, power off and on. Rocket engine equipped with original nozzles.

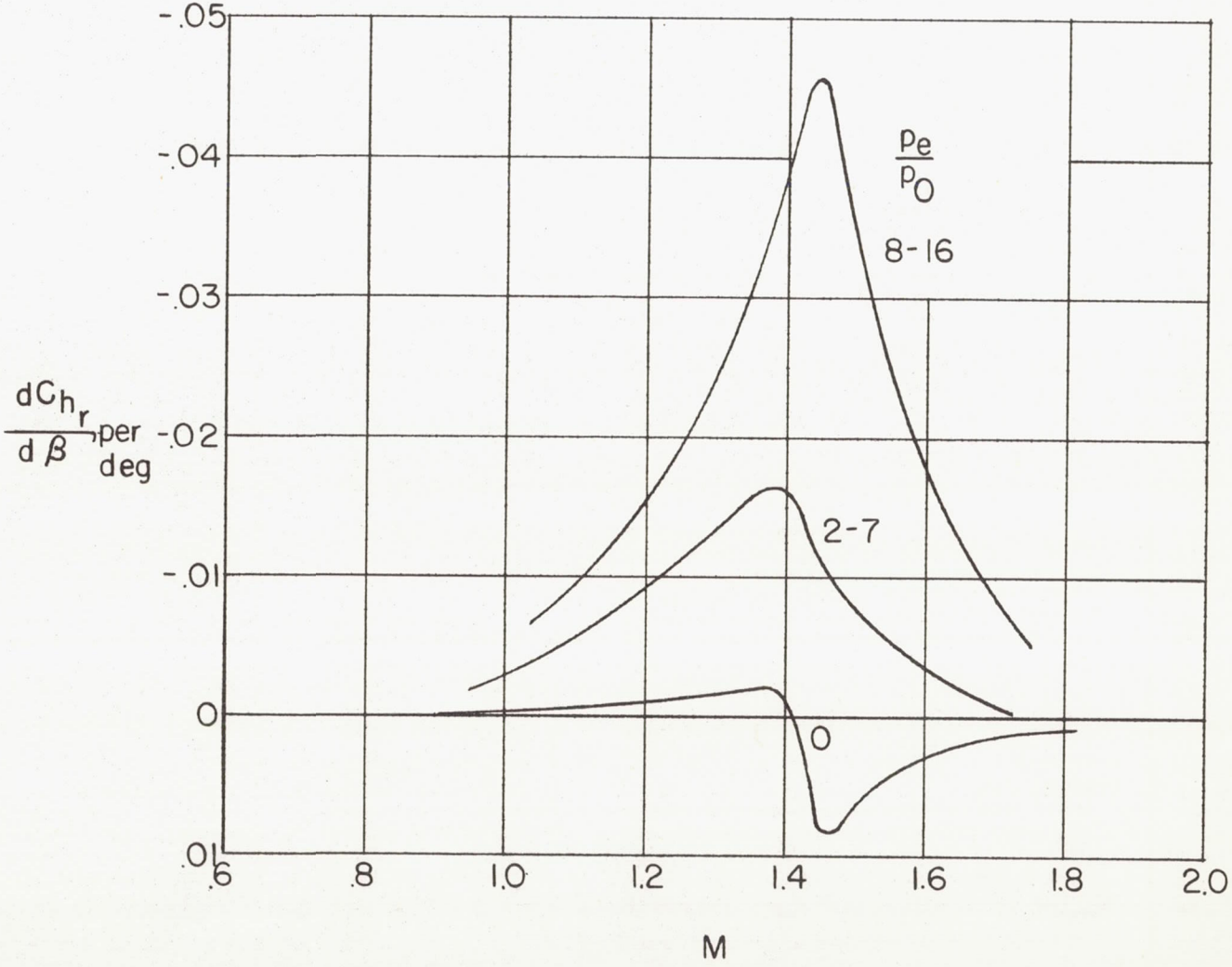

Figure 15.- Approximate variation of rudder hinge-moment parameter with Mach number at different pressure ratios.